M&C 2017 - International Conference on Mathematics & Computational Methods Applied to Nuclear Science & Engineering, Jeju, Korea, April 16-20, 2017, on USB (2017)

Application of the adjoint spectral Green's function–constant nodal method for one–speed X, Y–geometry discrete ordinates source–detector problems

Jesús Pérez Curbelo, † Ricardo C. Barros†

†*Instituto Politécnico, Universidade do Estado do Rio de Janeiro, P.O. Box 97282, 28610–974 Nova Friburgo, RJ, Brazil*
jcurbelo86@gmail.com, rcbarros@pq.cnpq.br

Abstract - *We present in this paper the application of the adjoint technique for solving one–speed X, Y–geometry discrete ordinates (S_N) transport problems by using a spectral–nodal method. We describe the spectral Green's function–constant nodal (Adjoint–SGF–CN) scheme and its new features, and compare the involved quantities with those appearing in the SGF–CN method for forward problems. The resulting Adjoint–SGF–CN equations are solved by using the adjoint partial one–node block inversion (NBI) iterative scheme. Numerical results are given to illustrate the method's features and some advantages of using the adjoint technique in source–detector problems.*

I. INTRODUCTION

The solution of the equation which is adjoint to the Boltzmann transport equation can be viewed as a measure of the importance of a particle to the objective function, e.g., a detector response [1]. This physical interpretation makes the adjoint flux well suited for use as a function of importance in deep penetration problems.

In this work we present a coarse–mesh method for one–speed X, Y–geometry discrete ordinates (S_N) adjoint transport problems considering isotropic scattering in non–multiplying media. In this method, the adjoint spectral Green's function (Adjoint–SGF) scheme, originally developed for solving adjoint S_N problems in slab–geometry with no spatial truncation error [2], is applied to solve the adjoint one–dimensional transverse–integrated S_N nodal equations with constant approximation for the terms corresponding to the transverse leakages in the forward problem. A companion method has been successfully applied to X, Y–geometry forward S_N problems [3]. It is well known that the S_N equations are not only non self–adjoint, but also have non self–adjoint boundary conditions. Nevertheless, we remark that if we use numerical methods for forward S_N problems with adjoint isotropic sources and vacuum or reflective boundary conditions, as it is applicable, we shall obtain the forward angular fluxes in the opposite directions of motion. Although this can be done in practical applications, we describe in this paper the present Adjoint–SGF–CN method, which has two new ingredients: (i) the adjoint auxiliary equation that we present in Section III.; and (ii) the adjoint partial one–node block inversion (NBI) iterative scheme, that we describe in section Section IV..

Numerical results to two source–detector test problems are considered in Section V. and Section VI. offers a number of general concluding remarks and suggestions for future work.

II. THE TRANSVERSE–INTEGRATED ADJOINT S_N CONSTANT–NODAL EQUATIONS

Let us consider the one–speed adjoint S_N equations in a rectangular domain $D = \{(x, y) \in \mathbb{R}^2 | 0 \le x \le L; 0 \le y \le H\}$ with isotropic scattering in non–multiplying media

$$-\mu_m \frac{\partial \psi_m^\dagger(x,y)}{\partial x} - \eta_m \frac{\partial \psi_m^\dagger(x,y)}{\partial y} + \sigma_T(x,y)\,\psi_m^\dagger(x,y) = \frac{\sigma_{S0}}{4}(x,y)\sum_{n=1}^{M}\psi_n^\dagger(x,y)\,\omega_n + Q^\dagger(x,y) \quad , \quad m = 1:M \quad , M = N(N+2)/2\,, \quad (1)$$

wherein non–outgoing adjoint flux boundary conditions apply, meaning that the importance of the leakage is clearly equal to zero, since such particles will not return to D, and thus, will not contribute to the detector response. In Eq (1) we have defined $\psi_m^\dagger(x, y)$ as the adjoint angular flux in direction (μ_m, η_m) and N is the order of the angular quadrature set. The ordered pair (μ_m, η_m) represents the discrete directions and ω_m are the corresponding weights. In addition, σ_T is the total macroscopic cross section and σ_{S0} is the isotropic scattering macroscopic cross section. The quantity $Q^\dagger(x, y)$ is the adjoint interior source, which is perfectly arbitrary [4]. Now we consider a rectangular spatial grid on D where each discretization node is denoted as $d_{i,j}$ of width h_{xi} and height h_{yj}. We also assume that the material parameters and the adjoint interior source are constant functions in $d_{i,j}$.

In order to obtain the one–dimensional transverse-integrated adjoint S_N nodal equations, we define the generalized transverse–integration operator

$$L_u = \frac{1}{h_{us}} \int_{u_{s-1/2}}^{u_{s+1/2}} \cdot\, du \quad , \quad (2)$$

where $u = x$ or y, and $s = i$ or j, respectively. First we apply L_y and then L_x to Eq. (1) within $d_{i,j}$ and obtain the one–dimensional transverse–integrated adjoint S_N nodal equations for the x and y coordinate directions, respectively. That is

$$-\frac{\mu_m}{\sigma_{T\,i,j}}\frac{d\widetilde{\psi}_{m,j}^\dagger(x)}{dx} + \widetilde{\psi}_{m,j}^\dagger(x) = \frac{c_{0\,i,j}}{4}\sum_{n=1}^{M}\widetilde{\psi}_{n,j}^\dagger(x)\,\omega_n + \frac{1}{\alpha_{m\,ij}^{y}}\left[\psi_m^\dagger(x, y_{j+1/2}) - \psi_m^\dagger(x, y_{j-1/2})\right] + \frac{Q_{i,j}^\dagger}{\sigma_{T\,i,j}} \quad (3)$$

and

$$-\frac{\eta_m}{\sigma_{T\,i,j}}\frac{d\widehat{\psi}^{\dagger}_{m,i}(y)}{dy}+\widehat{\psi}^{\dagger}_{m,i}(y)=\frac{c_{0\,i,j}}{4}\sum_{n=1}^{M}\widehat{\psi}^{\dagger}_{n,i}(y)\,\omega_n + \frac{1}{\alpha^{x}_{m\,ij}}\left[\psi^{\dagger}_{m}(x_{i+1/2},y)-\psi^{\dagger}_{m}(x_{i-1/2},y)\right]+\frac{Q^{\dagger}_{i,j}}{\sigma_{T\,i,j}} \quad , \quad (4)$$

where we have defined $\alpha^{y}_{m\,ij}\equiv\frac{h_{yj}\,\sigma_{T\,i,j}}{\eta_m}$, $\alpha^{x}_{m\,ij}\equiv\frac{h_{xi}\,\sigma_{T\,i,j}}{\mu_m}$ and the isotropic scattering ratio $c_{0\,i,j}\equiv\sigma_{S0\,i,j}/\sigma_{T\,i,j}$. In addition we define the averages of the adjoint angular fluxes over each spatial coordinate direction within node $d_{i,j}$

$$\widetilde{\psi}^{\dagger}_{m,j}(x)=\frac{1}{h_{yj}}\int_{y_{i-1/2}}^{y_{i+1/2}}\psi^{\dagger}_{m}(x,y)\,dx \quad (5)$$

and

$$\widehat{\psi}^{\dagger}_{m,i}(y)=\frac{1}{h_{xi}}\int_{x_{i-1/2}}^{x_{i+1/2}}\psi^{\dagger}_{m}(x,y)\,dx \quad . \quad (6)$$

Equations (3) and (4) form a system of $2M$ ordinary differential equations in $6M$ unknowns. Therefore, we need to introduce approximations to guarantee uniqueness of the solution. In this paper we approximate the adjoint node–edge angular fluxes in Eqs (3) and (4) by the adjoint node–edge average angular fluxes. That is

$$\psi^{\dagger}_{m}(x,y_{j\pm1/2})\approx\widehat{\psi}^{\dagger}_{m,i,j\pm1/2} \quad (7a)$$

and

$$\psi^{\dagger}_{m}(x_{i\pm1/2},y)\approx\widetilde{\psi}^{\dagger}_{m,i\pm1/2,j} \quad . \quad (7b)$$

Now, we substitute Eqs. (7a) and (7b) into Eqs. (3) and (4), respectively. For the x direction we obtain

$$-\frac{\mu_m}{\sigma_{T\,i,j}}\frac{d\widetilde{\psi}^{\dagger}_{m,j}(x)}{dx}+\widetilde{\psi}^{\dagger}_{m,j}(x)=\frac{c_{0\,i,j}}{4}\sum_{n=1}^{M}\widetilde{\psi}^{\dagger}_{n,j}(x)\,\omega_n + \frac{1}{\alpha^{y}_{m\,ij}}\left[\widehat{\psi}^{\dagger}_{m,i,j+1/2}-\widehat{\psi}^{\dagger}_{m,i,j-1/2}\right]+\frac{Q^{\dagger}_{i,j}}{\sigma_{T\,i,j}} \quad , m=1:M\,. \quad (8)$$

An analogous result is obtained for the y direction. Henceforth we shall perform our description only for the x direction, since similar results are obtained for the y direction.

At this point we solve Eq. (8) analytically, whose general solution can be written as

$$\widetilde{\psi}^{\dagger}_{m\,j}(x)=\widetilde{\psi}^{\dagger\,P}_{m\,j}+\widetilde{\psi}^{\dagger H}_{m\,j}(x) \quad , \quad x\in d_{i,j} \quad .$$

Here $\widetilde{\psi}^{\dagger\,P}_{m\,j}$ is a particular solution and $\widetilde{\psi}^{\dagger H}_{m\,j}(x)$ is the homogeneous component of the general solution. Substituting the spatially constant $\widetilde{\psi}^{\dagger\,P}_{m\,j}$ into Eq. (8) we obtain

$$\widetilde{\psi}^{\dagger\,P}_{m\,j}=\frac{Q^{\dagger}_{ij}}{\sigma_{T\,ij}\,(1-c_{0\,ij})}+\frac{c_{0\,ij}\;\Delta\widehat{J}^{\dagger}_{j}}{\sigma_{T\,ij}\,h_{yj}\,(1-c_{0\,ij})}+\widehat{\tau}^{\dagger}_{m\,ij} \quad , \quad (9)$$

where we have defined

$$\Delta\widehat{J}^{\dagger}_{j}\equiv\frac{1}{4}\sum_{n=1}^{M}\eta_n\,\omega_n\left(\widehat{\psi}^{\dagger}_{n,i,j+1/2}-\widehat{\psi}^{\dagger}_{n,i,j-1/2}\right)$$

and

$$\widehat{\tau}^{\dagger}_{m\,ij}\equiv\frac{1}{\alpha^{y}_{m\,ij}}\left(\widehat{\psi}^{\dagger}_{n,i,j+1/2}-\widehat{\psi}^{\dagger}_{n,i,j-1/2}\right) \quad .$$

To determine the homogeneous component, we consider the expression

$$\widetilde{\psi}^{\dagger H}_{mj}(x)=a^{\dagger}_{m}(\xi)\,e^{\frac{-\sigma_{T\,ij}(x-\lambda_i)}{\xi}}\;,\;\lambda_i=\begin{cases}x_{i+1/2} & ,\xi<0\\ x_{i-1/2} & ,\xi>0\end{cases}\;. \quad (10)$$

We remark that the shifting strategy considered in Eq. (10) with λ_i, so defined, is not essential, but prevents overflow disruption due to computational finite arithmetic in coarse–mesh calculations. Substituting Eq. (10) into the homogeneous equation corresponding to Eq. (8), we obtain

$$\sum_{n=1}^{M}\left\{-\frac{\delta_{m,n}}{\mu_m}+\frac{c_{0\,ij}\,\omega_n}{4\,\mu_m}\right\}a^{\dagger}_{n}(\xi)=\frac{1}{\xi}\,a^{\dagger}_{m}(\xi) \quad , \quad (11)$$

where $\delta_{m,n}$ is the *Kronecker delta*. For $m=1:M$, Eq. (11) represents an eigenvalue problem. Therefore, for $x\in d_{ij}$ we obtain a linearly independent set of M eigenfunctions defined in Eq. (10) and we write the general solution for Eq. (8) in node d_{ij} as

$$\widetilde{\psi}^{\dagger}_{m}(x)=\sum_{k=1}^{M}\beta_k\;a^{\dagger}_{m}(\xi_k)\;e^{\frac{-\sigma_{T\,ij}(x-\lambda_i)}{\xi_k}}+\widetilde{\psi}^{\dagger\,P}_{m\,j} \quad . \quad (12)$$

Here $a^{\dagger}_{m}(\xi_k)$ is the $m'th$ component of the eigenvector corresponding to the eigenvalue ξ_k^{-1}; β_k are arbitrary constants and $\widetilde{\psi}^{\dagger\,P}_{m\,j}$ is calculated by Eq. (9). Henceforth, we refer to ξ_k as an eigenvalue, although, in fact, the eigenvalue is ξ_k^{-1}, as we see in Eq. (11).

We remark at this point that the eigenvalues ξ_k for the adjoint transverse–integrated S_N equations in node d_{ij} appear in ± pairs due to the symmetry of the angular quadrature sets and they are all real numbers for the cases where $c_{0\,ij}<1$. Moreover, these eigenvalues are exactly the same as the eigenvalues for the corresponding forward transverse–integrated S_N equations in node d_{ij} [3]. On the other hand, the corresponding eigenvectors are all different, but they may have the same entries located in different positions within the column matrix, as represented in Fig. 1.

Figure 1 illustrates that, if we obtain the M–dimensional eigenvectors $a_m(\xi_k)$ corresponding to the simple eigenvalue ξ_k (multiplicity equal to one), by following a spectral analysis of the forward S_N nodal equations integrated in the y direction [3], viz Fig. 1a, then the eigenvectors $a^{\dagger}_{m}(\xi_k)$ corresponding to the same simple eigenvalue ξ_k for the adjoint S_N equations (8) interchange the first and second $M/4$–dimensional arrays as well as the third and fourth $M/4$–dimensional arrays, viz Fig. 1b. On the other hand, for the forward and adjoint S_N nodal equations integrated in the x direction, the eigenvectors corresponding to a given simple eigenvalue ξ_k do interchange

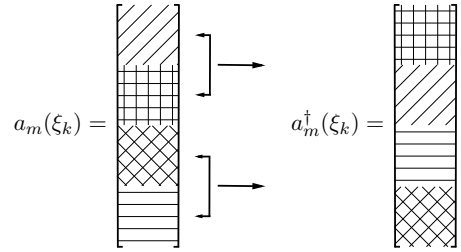

(a) Forward problem (b) Adjoint problem

Fig. 1: M–dimensional eigenvectors corresponding to the same simple eigenvalue ξ_k for the forward and adjoint S_N models integrated in the y direction within node d_{ij}, cf. Eq. (8).

the first and third in addition to the second and fourth $M/4$–dimensional arrays. This result is due to the change of signs of the discrete ordinates μ_m and η_m.

However, for the isotropic case, we obtain $M - N$ eigenvalues ξ_k equal to the values of μ_m (or η_m) according to the forward transverse–integrated S_N equations in y (or x) coordinate direction. These eigenvalues have multiplicity equal to $N - 2m + 1$ for $\mu_1 < \mu_2 < \ldots < \mu_{N/2}$. For example, if we use the S_6 model, we obtain one simple eigenvalue equal to μ_3, three eigenvalues equal to μ_2 and five eigenvalues equal to μ_1. Similar results are obtained for the case considering transverse–integration in the x direction, wherein the eigenvalues are equal to η_m with multiplicity also equal to $N-2m+1$ for $\eta_1 < \eta_2 < \ldots < \eta_{N/2}$. Furthermore, for the adjoint transverse–integrated S_N equations in y (or x) coordinate direction, one obtains the same $M - N$ eigenvalues with the same multiplicities. However, the corresponding eigenvectors are different for the forward and adjoint problems. For the transverse integration in the y direction, the eigenvectors corresponding to the same eigenvalue μ_m with multiplicity $N - 2m + 1 > 1$, $m = 1 : N/2 - 1$, may be linear combinations of the linearly independent eigenvectors corresponding to the same eigenvalue μ_m, with the same interchanges as illustrated in Fig. 1.

In the next section, we derive the Adjoint–SGF–CN method that preserves the local general solution of the transverse–integrated adjoint S_N nodal equations inside each node d_{ij}. Using boundary conditions and continuity conditions, we apply the Adjoint–SGF–CN method to solve numerically adjoint S_N problems on arbitrary rectangular grids.

III. THE ADJOINT SPECTRAL GREEN'S FUNCTION CONSTANT–NODAL METHOD

Integrating Eq. (1) within an arbitrary spatial cell d_{ij} by using the operator

$$\frac{1}{h_{xi}\,h_{yj}}\int_{x_{i-1/2}}^{x_{i+1/2}}\int_{y_{j-1/2}}^{y_{j+1/2}}(\cdot)\,dy\,dx \quad ,$$

we obtain the discretized adjoint spatial balance S_N equations

$$-\frac{4\mu_m}{h_{xi}}\Delta\widetilde{\psi}^\dagger_{mi}-\frac{4\eta_m}{h_{yj}}\Delta\widehat{\psi}^\dagger_{mj}+4\,\sigma_{T\,ij}\overline{\Psi}^\dagger_{m,j}=\sigma_{S0\,ij}\sum_{n=1}^{M}\overline{\psi}^\dagger_{n\,ij}\,\omega_n+4\,Q^\dagger_{ij}, \tag{13}$$

where we have defined

$$\Delta\widetilde{\psi}^\dagger_{mi}\equiv\widetilde{\psi}^\dagger_{m,i+1/2,j}-\widetilde{\psi}^\dagger_{m,i-1/2,j} \quad ,\Delta\widehat{\psi}^\dagger_{mj}\equiv\widehat{\psi}^\dagger_{m,i,j+1/2}-\widehat{\psi}^\dagger_{m,i,j-1/2}$$

and the node–average adjoint angular flux in cell Ω_{ij}

$$\overline{\Psi}^\dagger_{m,i,j}=\frac{1}{h_{xi}\,h_{yj}}\int_{x_{i-1/2}}^{x_{i+1/2}}\int_{y_{j-1/2}}^{y_{j+1/2}}\psi^\dagger_m(x,y)\,dydx \quad . \tag{14}$$

Equation (13), within an arbitrary spatial cell d_{ij}, represents a system of M algebraic linear equations in $3M$ unknowns. Therefore, we need to use $2M$ auxiliary equations. In the Adjoint–SGF–CN method we use an auxiliary equation of the form

$$\overline{\Psi}^\dagger_{m,i,j}=\sum_{\mu_n<0}\Lambda^{i,j}_{m,n}\,\widetilde{\psi}^\dagger_{n,j-1/2}+\sum_{\mu_n>0}\Lambda^{i,j}_{m,n}\,\widetilde{\psi}^\dagger_{n,j+1/2}+\widehat{G}_{m,i,j}(Q^\dagger_{ij}) \quad , \tag{15}$$

where $\widehat{G}_{m,i,j}(Q^\dagger_{ij})$ is a function of the interior adjoint source to be determined such that the particular solution is automatically preserved. To determine the term $\widehat{G}_{m,i,j}(Q^\dagger_{ij})$ we substitute Eq. (9) into Eq. (15) and the result appears as

$$\widehat{G}_{m,i,j}(Q^\dagger_{ij})=\sum_{n=1}^{N}\left(\delta_{m,n}\;-\;\Lambda^{i,j}_{m,n}\right)\widetilde{\psi}^{\dagger\,P}_{m\,j} \quad .$$

We determine the parameters $\Lambda^{i,j}_{m,n}$ by requiring that the homogeneus component of the local general solution be preserved by using equation (10) in equation (15) and, after some algebraic manipulations, we obtain the following linear systems:

$$\frac{\xi_k a^\dagger_m(\xi_k)}{\sigma_{Tij}h_{xi}}\left(1-e^{-\frac{\sigma_{Tij}h_{xi}}{\xi_k}}\right)$$
$$=\sum_{\mu_n<0}a^\dagger_n(\xi_k)\Lambda^{i,j}_{m,n}+e^{-\frac{\sigma_{Tij}h_{xi}}{\xi_k}}\sum_{\mu_n>0}a^\dagger_n(\xi_k)\Lambda^{i,j}_{m,n}\;,\quad(\xi_k>0) \tag{16}$$

and

$$\frac{|\xi_k|a^\dagger_m(\xi_k)}{\sigma_{Tij}h_{xi}}\left(1-e^{-\frac{\sigma_{Tij}h_{xi}}{|\xi_k|}}\right)$$
$$=e^{-\frac{\sigma_{Tij}h_{xi}}{|\xi_k|}}\sum_{\mu_n<0}a^\dagger_n(\xi_k)\Lambda^{i,j}_{m,n}+\sum_{\mu_n>0}a^\dagger_n(\xi_k)\Lambda^{i,j}_{m,n}\;,\quad(\xi_k<0). \tag{17}$$

Requiring this to hold for $m = 1 : M$ and $k = 1 : M$, we obtain a linear system of M^2 equations in the M^2 unknowns $\Lambda^{i,j}_{m,n}$.

We note that the present adjoint auxiliary equation (15) and the analogous one for the y direction are very similar to the auxiliary equation used for the forward SGF–CN method [3]. However, in the present Adjoint–SGF–CN method, the adjoint node–average angular flux in direction (μ_m, η_m) is related to the adjoint node–average angular fluxes in all outward directions and interior adjoint source, as opposed to the inward directions for the forward S_N problems. Therefore, the parameters $\Lambda^{i,j}_{m,n}$ can be viewed as the weights of the contributions of the outgoing particles through the node–edges, which have importances $\widetilde{\psi}^\dagger_{n,j\pm1/2}$ to the node–average importance of particles travelling in direction (μ_m, η_m), given by $\overline{\Psi}^\dagger_{m,i,j}$, for the detector response, that depends on the numerical value attributed to the adjoint source $Q^\dagger_{ij}$, normally equal to the macroscopic absorption cross section. Clearly the outgoing particles have non–zero importance to the detector response, since they might come back to node $d_{i,j}$, except if they leave the domain, as we have mentioned in Section II..

IV. ADJOINT PARTIAL ONE–NODE BLOCK INVERSION (NBI) ITERATIVE SCHEME

In order to generate numerical solutions of the Adjoint–SGF–CN equations, we use the adjoint partial one–node block inversion (NBI) iterative scheme. This iterative scheme uses the most recent available estimates for the outgoing adjoint node–edge average angular fluxes (solid arrows in Fig. 2), to solve the resulting adjoint S_N problem in that cell for all the incoming adjoint node–edge average angular fluxes in the opposite sweeping direction (dashed arrows in Fig. 2), which constitute the outgoing adjoint node–edge average angular fluxes for the adjacent cell in the sweeping direction. Each arrow in Fig. 2 represents $N(N+2)/8$ directions in each quadrant for the ①–③ sweeping direction.

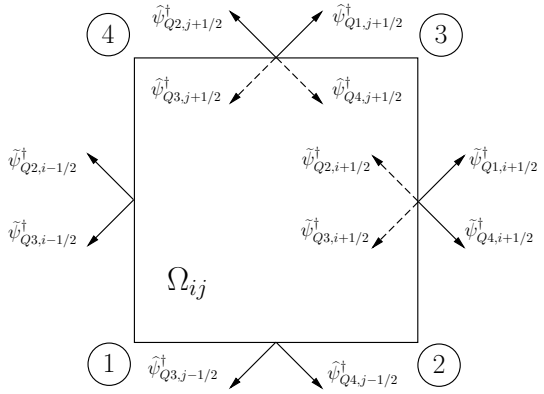

Fig. 2: Sweeping scheme for adjoint partial NBI algorithm in the ①–③ direction .

The algorithm is based on iterating on the node–edge average angular quantities in four sweeping directions: ①–③, ③–①, ②–④ and ④–② . Therefore, we substitute the Adjoint–SGF auxiliary equation (15) and the corresponding for the *y* coordinate direction into the balance equation (13) to remove the node–average angular quantities.

In the following section, we present numerical results illustrating the performance of the Adjoint–SGF–CN method with the adjoint partial NBI iterative scheme.

V. NUMERICAL RESULTS

In this section we consider two model problems. The first model problem consists of a uniform isotropic neutron source (Q_1) surrounded by a shielding material ($Q_2 = 0$). Figure 3 represents one–fourth of the whole shielding structure. The second model problem is a typical well–logging problem and we simulate the response for the detector D due to three sources located in different positions. Both model problems are are adapted from [5] and [6] and we compared the results by solving the forward problem and using the adjoint technique. The stopping criterion for each run required that the discrete maximum norm of the relative deviation between two consecutive estimates for the node–average scalar fluxes (forward and adjoint) did not exceed 10^{-6}. All numerical results were obtained by using a computational tool developed with the programming language *C++* (*Embarcadero ® C++ Builder XE2*).

1. Model Problem Nº 1

Let us consider a uniform isotropic neutron source ($Q_1 = 1\,cm^{-3}\,s^{-1}$) surrounded by a shielding material ($Q_2 = 0$) as represented in Fig. 3. Here we consider reflective boundary conditions for both left and bottom boundaries and prescribed boundary conditions for both right and upper boundaries.

In this work we simulate the detection of neutrons by two identical detectors D_1 and D_2 ($\sigma_A = 1.9\,cm^{-1}$) located as illustrated in Fig. 3. To solve the adjoint problem, we set the adjoint sources numerically equal to the detector absorption macroscopic cross section (σ_A), i.e., $Q^{\dagger} = 1.9$, and ran the two adjoint problems using the offered Adjoint–SGF–CN method with D_1 and D_2 separately.. Assuming prescribed boundary conditions for the forward S_N problem and zero outgoing adjoint flux boundary conditions for the adjoint S_N problem at the top and right boundaries of Fig. 3, the detector response can be obtained by

$$R = \langle \psi^{\dagger}, Q \rangle + \int_{\Gamma} d\Gamma \int_{\widehat{n}\cdot\widehat{\Omega}<0} d\widehat{\Omega}\ \ |\widehat{n}\circ\widehat{\Omega}|\ \ \psi^{\dagger}\left(\boldsymbol{r}_{\Gamma}, \widehat{\Omega}\right)\ \ \Psi\left(\boldsymbol{r}_{\Gamma}, \widehat{\Omega}\right) \quad . \tag{18}$$

where we have defined the integral operation [7]

$$\langle \cdot, \cdot \rangle \equiv \int_{\Gamma} d\Gamma \int_{4\pi} d\Omega \quad .$$

Here Γ is the contour surface and Ω is the direction of motion.

We used the LQ_{16} angular quadrature set [7] and two spatial grids. The results for the forward problem were obtained by using the forward SGF–CN method [3].

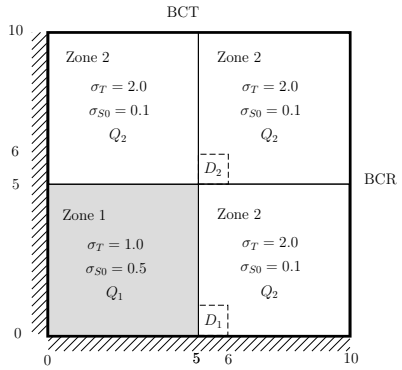

Fig. 3: Geometry and nuclear data for Model Problem Nº 1.

Table II shows the results for the detector response obtained by running both the forward and adjoint methods. The third and fourth columns display the absorption rate densities for detectors D_1 and D_2, respectively. We remark that the adjoint technique yields the detector response due to the interior source and/or to the incoming boundary conditions by running the Adjoint–SGF–CN method only once. On the other hand, if it is required this information by solving the forward problem, the code must be run at least twice. As we see, in all cases, the results (including interior source and the boundary conditions) generated with forward and adjoint techniques do agree, at least, up to the sixth decimal place. We emphasize that the use

of the adjoint technique to calculate the detector response is convenient as it is possible to use the same adjoint solution for various distinct intensities and/or locations of the interior sources and/or type of boundary conditions, provided we do not change the location and the type of the detector.

20×20 [a]		R_1 $(cm^{-1}\, s^{-1})$ [b]	R_2 $(cm^{-1}\, s^{-1})$ [b]
Forward	$\{1;1;2\}$ [c]	3.95677×10^{-1}	6.83531×10^{-2}
Adjoint	$\{1;0;0\}$	3.95647×10^{-1}	6.83082×10^{-2}
	$\{0;1;2\}$	3.04653×10^{-5}	4.49492×10^{-5}
	$\{1;1;2\}$	3.95677×10^{-1}	6.83531×10^{-5}
40×40 [a]			
Forward	$\{1;1;2\}$ [c]	3.95694×10^{-1}	6.86079×10^{-2}
Adjoint	$\{1;0;0\}$	3.95663×10^{-1}	6.85629×10^{-2}
	$\{0;1;2\}$	3.04652×10^{-5}	4.50485×10^{-2}
	$\{1;1;2\}$	3.95694×10^{-1}	6.86079×10^{-2}

[a] Spatial grid: Number of nodes in the x direction $\times$ number of nodes in the y direction.
[b] Absortion rate density per unit length.
[c] $\{Q; BCT; BCR\}$: numerical values of the interior source Q and the isotropic boundary conditions on the top and the right–hand side boundaries, viz. Fig. 3.

TABLE I: Neutron detection for the Model Problem Nº 1.

Figures 4 and 5 shows the distributions of the importance functions of neutrons from an adjoint source at the detector position D_1 and D_2, respectively. Clearly, high importance values appear near the adjoint sources.

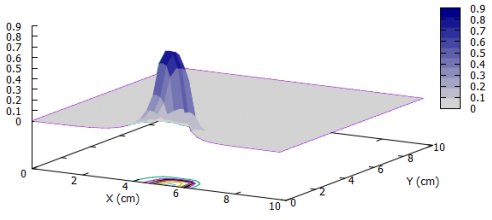

Fig. 4: Importance function distribution for the Model Problem Nº 1. (adjoint source D_1).

2. Model Problem Nº 2

The second model problem represents an oil well–logging problem for geophysics applications. This model problem was considered in [5] and [6], where one numerical experiment consisted in calculating the average scalar flux in region D_1 due to an isotropic unit source located in region Q_1 (Fig. 6). The geometry and nuclear data for this test problem are shown in Fig. 6.

In this model problem we consider four numerical experiments to illustrate the efficiency of the adjoint technique for the source–detector transport calculations. To solve the adjoint problem we used the present Adjoint–SGF–CN method on spatial grids composed of 56×64 and 112×128 nodes with the

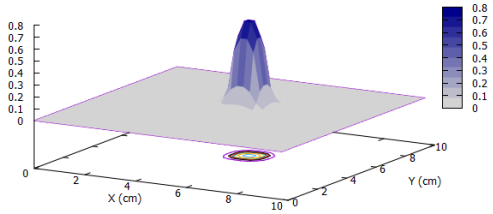

Fig. 5: Importance function distribution for the Model Problem Nº 1. (adjoint source D_2).

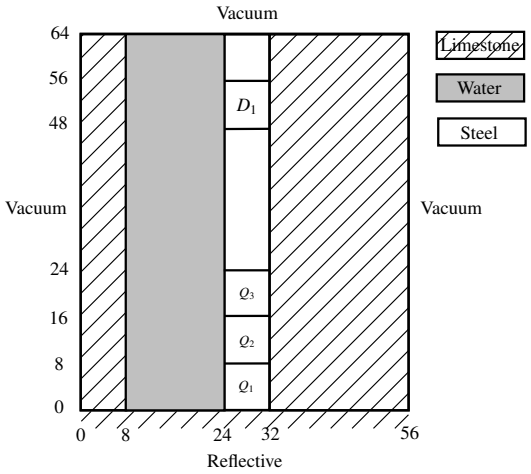

Fig. 6: Geometry and material distribution for Model Problem Nº 2. Limestone ($\{\sigma_T;\ \sigma_{S0}\}$) = {0.330263; 0.314419}, water = {0.694676; 0.634883} and steel = {0.499122; 0.314419}. Width = 56 cm and height = 64 cm.

level symmetric S_6 and S_{16} angular quadrature sets [7]. For these experiments we also set the adjoint source numerically equal to the detector absorption macroscopic cross section; ie., $Q^{\dagger} = 0.004662$ and ran the adjoint problem considering reflective boundary conditions at the bottom and zero outgoing adjoint angular fluxes at the other three boundaries [7]. Table II displays the numerical results for the D_1 detector response due to a unit source Q_1, and then Q_2, and then Q_3 independently and all together. We remark that we ran the Adjoint–SGF–CN code only once and then used the adjoint numerical solution in Eq. (18) to evaluate the detector response for each experiment. This was possible because the detector was not changed nor displaced.

On the other hand, if we were to run the forward S_N problems, we should run four times the forward SGF–CN code, one for each location of the unit source in Fig. 6 and one for all the three sources together, apart from the fact that the latter is just the sum of the former three detector readings. As we see, the results are very accurate with respect to the forward calculations. Figure 7 shows the importance function distribution for this model problem. As we see, the particles

56×64 [a]		S_6 [b]	S_{16} [b]
Forward	$\{1;1;1\}$ [c]	4.31868×10^{-2}	4.32747×10^{-2}
Adjoint	$\{1;0;0\}$	3.01619×10^{-2}	3.02205×10^{-2}
	$\{0;1;0\}$	9.33320×10^{-3}	9.35334×10^{-3}
	$\{0;0;1\}$	3.69181×10^{-3}	3.70093×10^{-3}
	$\{1;1;1\}$	4.31869×10^{-2}	4.32748×10^{-2}
112×128 [a]			
Forward	$\{1;1;1\}$ [c]	4.33938×10^{-2}	4.34765×10^{-2}
Adjoint	$\{1;0;0\}$	3.03046×10^{-2}	3.03596×10^{-2}
	$\{0;1;0\}$	9.37859×10^{-3}	9.39757×10^{-3}
	$\{0;0;1\}$	3.71067×10^{-3}	3.71930×10^{-3}
	$\{1;1;1\}$	4.33939×10^{-2}	4.34765×10^{-2}

[a] Spatial grid: Number of nodes in the x direction $\times$ number of nodes in the y direction.
[b] Level symmetric angular quadrature.
[c] $\{Q_1; Q_2; Q_3\}$: numerical values of the interior sources Q_1, Q_2 and Q_3, viz. Fig. 6.

TABLE II: Neutron detection R ($cm^{-1}\ s^{-1}$) for Model Problem Nº 2.

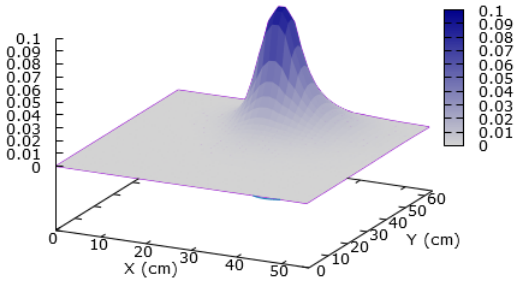

Fig. 7: Importance function distribution for Model Problem Nº 2. (adjoint source D_1).

that migrate close to the detector have more importance for the detector response than the ones that migrates farther.

VI. CONCLUDING REMARKS

We have developed a spectral nodal method, that we refer to as the Adjoint–SGF–CN method for monoenergetic adjoint S_N problems in X, Y–geometry. In this method, the only approximation involved is in the transverse leakage terms of the transverse–integrated adjoint S_N nodal equations. The terms involving the scattering events and the adjoint source are treated analytically.

A negative feature of the Adjoint–SGF–CN method is that it requires more storage than standard discretization methods. This is due to the fact that the NBI iterative scheme requires the storage of the node–edge average angular quantities. However, this extra storage requirement can be compensated by the possibility of using coarse spatial meshes.

According to the model problems considered in the previous section, the numerical results for the detector response, as generated with forward and adjoint techniques, were identical up to the sixth decimal place for the first problem and up to the fifth decimal place for the second problem. We note that the use of the adjoint technique to calculate the detector response is convenient as it is possible to run the adjoint problem just once, provided we do not change the location nor the type of the detector. We stress at this point that, even though we can generate adjoint S_N solution artificially by use of the forward S_N numerical methods, we offer in this paper an accurate nodal method for coarse–mesh, one–speed, adjoint S_N calculations in X, Y geometry with isotropic scattering.

We intend to apply these ideas to an arbitrary order L of scattering anisotropy and energy multigroup S_N problems in X, Y–geometry to account for the energy transfer in scattering events.

VII. ACKNOWLEDGMENTS

The authors acknowledge the financial support of the National Institute of Science and Technology on Innovative Nuclear Reactors, Brazil, for the ongoing development of this work. The work by Jesús Pérez Curbelo was supported by Fundação Coordenação de Aperfeiçoamento de Pessoal de Nível Superior (CAPES–Brazil) and Fundação Carlos Chagas Filho de Amparo à Pesquisa do Estado do Rio de Janeiro (FAPERJ–Brazil).

REFERENCES

1. G. I. BELL and S. GLASSTONE, *Nuclear Reactor Theory*, Van Nostrand Reinhold , New York, USA (1970).
2. D. S. MILITÃO, H. ALVES, and R. C. BARROS, "A numerical method for monoenergetic slab–geometry fixed–source adjoint transport problems in the discrete ordinates formulation with no spatial truncation error," *International Journal of Nuclear Energy Science and Technology*, **7**, *2*, 151–165 (2012).
3. R. C. BARROS and E. W. LARSEN, "A Spectral Nodal Method for One–Group X,Y–Geometry Discrete Ordinates Problems," *Nuclear Science and Engineering*, **111**, *1*, 34–45 (1992).
4. J. J. DUDERSTADT and W. R. MARTIN, *Transport Theory*, Wiley–Interscience, New York, USA (1979).
5. Y. Y. AZMY, "Comparison of three approximations to the linear–linear nodal transport method in weighted diamond–difference form," *Nuclear Science and Engineering*, **100**, 190–200 (1988).
6. D. S. DOMÍNGUEZ and R. C. BARROS, "The spectral Green's function linear-nodal method for one–speed X, Y–geometry discrete ordinates deep penetration problems," *Annals of Nuclear Energy*, **34**, *12*, 958–966 (2007).
7. E. E. LEWIS and W. F. MILLER, *Computational methods of neutron transport*, American Nuclear Society, Illinois, USA (1993).